In vitro transcribed guide RNAs trigger an innate immune response via the RIG-I pathway

Short title: *In vitro* transcribed guide RNAs trigger an innate immune response

Beeke Wienert[1,2], Jiyung Shin[1,2], Elena Zelin[1,2], Kathleen Pestal[2] and Jacob E. Corn[1,2,#]

[1] Innovative Genomics Initiative, University of California, Berkeley, Berkeley, USA

[2] Department of Molecular and Cell Biology, University of California, Berkeley, Berkeley, USA

[#] Corresponding author: jcorn@berkeley.edu

Abstract

CRISPR-Cas9 genome editing is revolutionizing fundamental research and has great potential for the treatment of many diseases. While editing of immortalized cell lines has become relatively easy, editing of therapeutically relevant primary cells and tissues can remain challenging. One recent advancement is the delivery of a Cas9 protein and an *in vitro* transcribed (IVT) guide RNA (gRNA) as a precomplexed ribonucleoprotein (RNP). This approach allows editing of primary cells such as T cells and hematopoietic stem cells, but the consequences beyond genome editing of introducing foreign Cas9 RNPs into mammalian cells are not fully understood. Here we show that the IVT gRNAs commonly used by many laboratories for RNP editing trigger a potent innate immune response that can be several thousand times stronger than benchmark immune stimulating ligands. IVT gRNAs are recognized in the cytosol through the RIG-I pathway but not the MDA5 pathway, thereby triggering a type I interferon response. Removal of the 5'-triphosphate from gRNAs ameliorates inflammatory signaling and prevents the loss of viability associated with genome editing in hematopoietic stem cells. The potential for Cas9 RNP editing to induce a potent antiviral response indicates that care must be taken when designing therapeutic strategies to edit primary cells.

Abbreviations:

Cas - CRISPR-associated

CIP - calf intestinal alkaline phosphatase

CRISPR - clustered, regularly interspaced, short palindromic repeat

dCas9 – nuclease-dead Cas9

HEK293 - Human embryonic kidney cells 293

HEK293T - Human embryonic kidney cells 293 SV40 large T antigen

HeLa – Henrietta Lacks cells

HSPCs – $CD34^+$ human hematopoietic stem and progenitor cells

IFNAR1 - Interferon Alpha And Beta Receptor Subunit 1

IFNβ/IFNB1 - Interferon beta

ISG15 - Interferon-stimulated gene 15

IVT – *in vitro* transcribed

KO - knockout

MAVS - mitochondrial activator of virus signaling

MDA5/IFIH1 - melanoma differentiation-associated gene 5/ Interferon Induced with Helicase C Domain 1

PAMP - pathogen-associated molecular pattern

RIG-I/DDX58 - retinoic acid-inducible gene I/ DExD-H-box helicase 58

gRNA –guide RNA

SPRI - solid phase reversible immobilization

WT – wild type

41 # Introduction

42 CRISPR (clustered, regularly interspaced, short palindromic repeat)-Cas (CRISPR-associated)
43 genome editing has rapidly become a widely used tool in molecular biology laboratories. Its ease
44 of use and high flexibility allows researchers to modify and edit genomes in cell lines (1), stem
45 cells (2), animals and plants (3,4), and even human embryos (5). At least two components must
46 be successfully delivered into cells during genome editing: the Cas protein, such as Cas9, and a
47 guide RNA (gRNA) to direct the Cas protein to its target site. For *in vitro* cultured cells this can
48 be done by transfecting plasmids encoding gRNA and Cas9 protein. However, transfection of
49 plasmid DNA into sensitive cell types such as primary and stem cells is challenging and inefficient.
50 The introduction of plasmids can also lead to undesired integration of DNA at the cut site (6),
51 increased off-target activity through prolonged expression of the CRISPR-Cas9 components (7),
52 and a delay in editing while the cell expresses gRNA and Cas protein (8).
53
54 The delivery of gRNA and Cas9 protein as a pre-complexed ribonucleoprotein (RNP) sidesteps
55 issues related to plasmid expression and has proved to be a successful strategy to edit human
56 primary cells, including T cells (9,10), hematopoietic stem cells (11–14), and neurons (15). This
57 makes RNP editing a particularly attractive approach for therapeutic applications, but relatively
58 little is known about the non-editing consequences of introducing a foreign gRNA and Cas9
59 protein. Human cells have evolved multiple defense mechanisms to guard against foreign
60 components, and genome editing reagents have the potential to activate these systems. For
61 example, recent data suggests that humans may have a pre-existing adaptive immune response to
62 the Cas9 protein (16). But cellular responses to the gRNAs used to program Cas9 editing have so
63 far not been well explored.

Cells respond to infection by RNA-viruses with an innate immune response that protects the host cell from invading foreign genetic material (17). Foreign RNAs are recognized by pathogen-associated molecular pattern (PAMP) binding receptors in the cytosol that include retinoic acid-inducible gene I (RIG-I) and melanoma differentiation-associated gene 5 (MDA5) (18). This triggers a cascade of events mediated by the mitochondrial activator of virus signaling (MAVS) protein resulting in the transcriptional activation of type I interferons and interferon-stimulated genes (ISGs) (19–21).

PAMPs usually contain exposed 5'-triphosphate ends (18), which may also be present in gRNAs made via T7 *in vitro* transcription (IVT) (22,23). We asked whether IVT gRNAs cause an innate immune response, and here show that RNP genome editing induces upregulation of interferon beta (IFNβ) and interferon-stimulated gene 15 (ISG15) in a variety of human cell types. This activity depends upon RIG-I and MAVS, but is independent of MDA5. The extent of the immune response depends upon the protospacer sequence, but removal of the 5'-triphosphate from gRNAs avoids stimulation of innate immune signaling. The potential for Cas9 RNP editing to induce an antiviral response indicates that care must be taken when designing therapeutic strategies to edit primary cells.

Results

To investigate if mammalian cells react to IVT gRNA/Cas9 with an innate immune response, we first performed genome editing in human embryonic kidney 293 (HEK293) cells using Cas9 RNPs. To separate innate immune response from genome editing, we performed these experiments with a non-targeting gRNA that recognizes a sequence within BFP and has no known targets within the

human genome (24). Constant amounts of recombinant Cas9 protein were complexed with different amounts of non-targeting IVT gRNA and RNPs were transfected into HEK293 cells using CRISPRMAX lipofection reagent (25). We harvested cells 30h after transfection and measured transcript levels of *IFNB1* and *ISG15* by qRT-PCR (**Figure 1A**). Introduction of gRNAs caused a dramatic increase in both *IFNB1* and *ISG15* levels, and the presence of Cas9 protein did not have an effect on the outcome. Cas9 on its own did not induce *IFNB1* or *ISG15* expression. To our surprise, as little as 1 pmol of gRNA was sufficient to trigger a 30-50-fold increase in the transcription of innate immune genes. We further found that the commonly-administered 100 pmol of a gRNA can induce *IFNB1* by 4,000 fold, which is equal to or even stronger than induction by canonical IFNβ inducers such as viral mRNA from Sendai Virus (26) or a Hepatitis C virus (HCV) PAMP (20,27) (**Figure 1B**).

RNPs can be delivered into cells via different transfection methods and while lipofection is cost-effective and easy to use, many researchers prefer electroporation for harder-to-transfect cells. We wondered if the transfection method would affect the IFNβ response and compared gRNA transfection via lipofection (Lipofectamine 2000 and RNAiMAX) to nucleofection (Lonza) (**Figure 1C**). Lipofection led to a strong increase in *IFNB1* and *ISG15* transcript levels after as little as 6h post transfection, and the response was sustained for up to 48 hours. Nucleofection also caused an increase in innate immune signaling at early time points, but the response was much milder than in lipofected samples and was greatly diminished by 48 hours.

Next, we asked if the innate immune response to gRNAs is a common phenomenon across different cell types and compared IFNβ activation in seven commonly used human cell lines of various

lineages: HEK293T, HEK293, HeLa, Jurkat, HCT116, HepG2 and K562 (**Figure 2A**). While the magnitude of induction varied between cell lines, all tested cell lines responded to IVT gRNA transfection with activation of *IFNB1* expression. The sole exception was K562 cells, which have a homozygous deletion of the *IFNA* and *IFNB1* genes (28). We also measured transcript levels of two major cytosolic pathogen recognition receptors, RIG-I (*DDX58*) and MDA5 (*IFIH1*), and noticed that all cell lines except K562 upregulated these transcripts in response to introduction of gRNAs. We also confirmed these results on the protein level in HEK293 cells (**Figure 2B**).

The RIG-I and MDA5 receptors complement each other by recognizing different structures in foreign cytosolic RNAs, but the exact nature of their ligands is not yet fully understood (29,30). To investigate if IVT gRNAs are recognized via RIG-I or MDA5, we generated clonal knockout (KO) cell lines for RIG-I, MDA5, and their downstream interaction partner MAVS in HEK293 cells using CRISPR-Cas9. As the expression of both RIG-I and MDA5 are themselves stimulated by IFNβ, we confirmed successful KO after transfection with gRNAs by genomic PCR, Sanger sequencing, and Western Blot (**Supplementary Figure 1A-C**). MAVS KO cells were confirmed by Western Blot (**Supplementary Figure 1D**). Strikingly, activation of *IFNB1 e*xpression after introduction of gRNAs was absent in RIG-I and MAVS KO cells, while MDA5 KO cells did not show a significant decrease in *IFNB1* transcript levels (**Figure 2C**). This indicates that IVT gRNAs are exclusively recognized through RIG-I to trigger a type I interferon response.

As the structural requirements of RIG-I ligands are still not completely understood, we wondered if different 20 nucleotide protospacers in gRNAs vary in their potency to trigger an innate immune response via RIG-I. We designed 10 additional non-targeting gRNAs that we *in vitro* transcribed

and transfected into HEK293 cells. Surprisingly, we found that the cells responded to different protospacers with a wide range of differential *IFNB1* expression. Several gRNAs produced very little innate immune response, and one gRNA (gRNA11) yielded no *IFNB1* activation at all (**Figure 3A**). We speculated that the differential response may be correlated with the purity of the RNA product after IVT or the stability of the secondary structure of the RNA (31). However, we found that there was no obvious correlation between the immune response to certain gRNAs and their purity, predicted protospacer secondary structure, full secondary structure including the constant region, or predicted disruption of the constant region by mis-pairing with the protospacer (**Supplementary Figure 2**). These results indicate that RIG-I recognition patterns of IVT gRNAs are complex and difficult to predict *a priori* based on predicted properties of the variable protospacer.

One well-established requirement of RIG-I ligands is the presence of a 5'-triphosphate group (32). We asked if preparations that remove the 5' triphosphate might avoid or reduce the innate immune response to IVT gRNAs. We first used a synthetic gRNA that lacks a 5'-triphosphate and verified that this gRNA does not induce *IFNB1* expression when transfected into HEK293 cells (**Figure 3B**). Synthetic guide RNAs are becoming more commonplace, but are still an order of magnitude more expensive than IVT of gRNAs. This limits their application for high-throughput interrogation of gene function in primary cells. We therefore asked if treatment of IVT gRNA with calf intestinal alkaline phosphatase (CIP) to remove the 5'-triphosphate would reduce *IFNB1* induction. We found that CIP treatment significantly reduced the *IFNB1* response (**Figure 3B**). Using different CIP treatment regimes, we further found that removal of the 5'-triphosphate must to be absolutely complete and should be carried out rigorously to avoid IFN stimulation (**Supplementary Figure**

A-B). We also compared purification of IVT gRNAs by solid phase reversible immobilization (SPRI) beads to column purification and established that SPRI bead clean-up is not sufficient to completely avoid an immune response even when more CIP is used (**Figure 3B and Supplementary Figure 3C**). Taken together, these results indicate that 5'-triphosphate is a necessary requirement for gRNA-induced *IFNB1* activation through RIG-I, but that additional structural properties of the gRNAs also influence the magnitude of the immune response.

When a cell initiates an antiviral immune response, it also undergoes cellular stress that can affect cell viability (33,34). Hence, we asked if there is a correlation between the IFNβ response and cell viability after transfection with synthetic, IVT or CIP-treated IVT gRNA. Not surprisingly, the viability of the very robust HEK293 cell line was not affected by the antiviral immune response (**Supplementary Figure 3D**). We then turned to primary $CD34^+$ human hematopoietic stem and progenitor cells (HSPCs), which are a much more sensitive cell type. We first nucleofected HSPCs with RNPs targeting the *HBB* gene (11) and compared synthetic and IVT gRNA interferon stimulation and cell viability post transfection. Double-strand breaks have been reported to cause innate immune stimulation and can themselves cause decreases in cell fitness (35,36). Therefore, we performed controls using nuclease-dead Cas9 (dCas9) to form RNPs. We saw a significant decrease in cell viability of HSPCs in both IVT gRNA RNP samples which was associated with an increase in IFN stimulated genes *ISG15* and *RIG-I* (**Figure 3C-D**). We did not see a substantial difference in viability or ISG expression between Cas9 and dCas9 RNPs suggesting that nuclease activity did not affect the immune response. Next, we asked if CIP treatment of gRNAs could reverse the decrease in viability in HSPCs. We nucleofected HSPCs with dCas9 RNPs targeting a

178 non-coding intron of *JAK2* and compared synthetic, IVT and CIP-treated IVT gRNAs. Strikingly,
179 CIP treatment could completely restore the viability in HSPCs (**Figure 3E**).
180

181 ## Discussion

182 We have found that IVT gRNAs used with Cas9 RNPs for many genome editing experiments can
183 trigger a strong innate immune response in many mammalian cell types (**Figure 4**). Lipofection
184 results in a stronger and longer lasting response than nucleofection, possibly because lipofection
185 delivers gRNAs to the cytosol while nucleofection delivers mainly to the nucleus. Using isogenic
186 knockout clones, we found the gRNA-induced response is mediated via the anti-viral RIG-I
187 pathway and results in expression of genes that initiate an antiviral immune response. While
188 introduction of IFN-stimulating gRNAs does not affect viability in HEK293 cells, we found that
189 viability of primary HSPCs is negatively affected by the antiviral immune response.
190

191 These results have several implications. We suggest that the gene signature associated with type I
192 interferon stimulation should be considered when studying the transcriptome of recently edited
193 bulk populations of cells. Furthermore, all mammalian cells can both produce type I interferons
194 and also respond to them through the ubiquitously expressed receptor Interferon Alpha And Beta
195 Receptor Subunit 1 (IFNAR1) (37). Even cells that have not been successfully transfected with
196 RNPs could sense the INFβ produced by neighboring cells and activate downstream antiviral
197 defense mechanisms. This could be an important consideration during *in vivo* genome editing
198 applications as RNP delivery into one set of cells could provoke a wide-spread innate immune
199 response in the surrounding tissues.
200

We found that synthetic gRNAs completely circumvent the RIG-I mediated response, offering a valuable path to avoid innate immune signaling during therapeutic editing. However, synthetic gRNAs can become expensive when performing experiments that require testing or using many gRNAs. We found that a cost-effective CIP treatment to remove the 5'-triphosphate before transfection reduces the immune response and increases post-transfection viability in HSPCs. Complete removal of the 5'-triphosphate is essential to restore viability in HSPCs to the same level as observed with synthetic gRNAs. Thus, consideration of a potential innate immune stimulation prior to choice of genome editing reagents, study design, and implementation of controls is critical when performing genome editing using RNPs in mammalian cells.

Double-strand breaks have on their own been reported to induce an innate immune response (35). However, we performed controls comparing WT Cas9 to a nuclease-dead Cas9 thereby showing that the gRNA-mediated innate immune response and associated cell death in HSPCs is not caused by double-strand breaks.

While we were preparing this manuscript for submission, the Kim group reported similar results in HeLa cells and primary human $CD4^+$ T cells (38). They confirmed that the type I interferon response is dependent on the presence of a 5'-triphopsphate group and that CIP treatment can increase viability by avoiding the antiviral response. These results are very much in alignment with our findings and extend the potential problem of innate immune signaling to additional cell types.

Our study adds extra depth by further outlining the mechanisms by which gRNAs are sensed. We show that gRNA sensing depends upon RIG-I and MAVS, but MDA5 knockout cells are fully capable of inducing IFNβ after IVT gRNA transfection. Hence, gRNA sensing is independent of

the MDA5 PAMP receptor. Furthermore, we show that in addition to a 5'-triphosphate, the protospacer sequence is also critical to determine the intensity of the IFNβ response. Not only do different gRNAs induce different innate immune responses, some gRNAs induce no response at all. It has been proposed that 5'-basepaired RNA structures are required to activate antiviral signaling via RIG-I, but we found no correlation between signaling and a variety of predicted RNA properties, including secondary structure (31). Our results therefore suggest that the mechanism of gRNA sensing by the RIG-I pathway is relatively complex, in that it requires 5' triphosphates but that this moiety is not sufficient to induce the response. Future work to delineate the full set of molecular features responsible for gRNA activation of innate immunity might yield accurate predictors of innate immune signaling in general.

Materials and methods

In vitro transcription of gRNAs

gRNA was synthesized by assembly PCR and *in vitro* transcription as previously described (11). Briefly, a T7 RNA polymerase substrate template was assembled by PCR from a variable 58-59 nt primer containing T7 promoter, variable gRNA guide sequence, and the first 15 nt of the non-variable region of the gRNA (T7FwdVar primers, 10 nM, Supplementary Table 1; Supplementary Table 2 for gRNA sequences), and an 83 nt primer containing the reverse complement of the invariant region of the gRNA (T7RevLong, 10 nM), along with amplification primers (T7FwdAmp, T7RevAmp, 200 nM each). The two long primers anneal in the first cycle of PCR and are then amplified in subsequent cycles. Phusion high-fidelity DNA polymerase was used for assembly (New England Biolabs). Assembled template was used without purification as a substrate for *in vitro* transcription by T7 RNA polymerase using the HiScribe T7 High Yield RNA Synthesis

kit (New England Biolabs) following the manufacturer's instructions. Resulting transcription reactions were treated with DNAse I (New England Biolabs), and RNA was purified by treatment with a 5X volume of homemade solid phase reversible immobilization (SPRI) beads (comparable to Beckman-Coulter AMPure beads) and elution in RNAse-free water.

CIP treatment of IVT gRNAs

When gRNAs were treated with Alkaline Calf intestinal phosphatase (CIP) (New England Biolabs), 20U of CIP (2 µl) were added per 20 µl IVT reaction and samples were incubated at 37C for 3h before proceeding to purification and DNAseI treatment. CIP-treated samples and corresponding no CIP IVT gRNA controls were purified using a Qiagen RNeasy Mini Kit (Qiagen). The detailed protocol and additional notes are available online (dx.doi.org/10.17504/protocols.io.nghdbt6).

In vitro transcription of HCV PAMP and Sendai Virus DI RNA

HCV PAMP IVT template (20) was generated by annealing HCV fwd and rev (5 µM each) oligos (Supplementary Table 1). 2 µl of the annealed product was used as DNA template in the subsequent IVT reaction using HiScribe T7 High Yield RNA Synthesis kit (New England Biolabs).

The plasmid containing the SeV DI RNA(26) was a gift from Prof. Peter Palese, Icahn School of Medicine at Mount Sinai, New York. Plasmid was digested with HindII/EcoRI before IVT with HiScribe T7 High Yield RNA Synthesis kit (New England Biolabs). The sequence of the IVT DI, including the T7 promoter, hepatitis delta virus ribozyme, and the T7 terminator, is:

269 TAATACGACTCACTATA**ACCAGACAAGAGTTTAAGAGATATGTATCCTTTTAAAT**

270 **TTTCTTGTCTTCTTGTAAGTTTTTCTTACTATTGTCATATGGATAAGTCCAAGAC**

271 **TTCCAGGTACCGCGGAGCTTCGATCGTTCTGCACGATAGGGACTAATTATTACG**

272 **AGCTGTCATATGGCTCGATATCACCCAGTGATCCATCATCAATCACGGTCGTGT**

273 **ATTCATTTTGCCTGGCCCCGAACATCTTGACTGCCCCTAAAATCTTCATCAAAA**

274 **TCTTTATTTCTTTGGTGAGGAATCTATACGTTATACTATGTATAATATCCTCAAA**

275 **CCTGTCTAATAAAGTTTTTGTGATAACCCTCAGGTTCCTGATTTCACGGGATGA**

276 **TAATGAAACTATTCCCAATTGAAGTCTTGCTTCAAACTTCTGGTCAGGGAATGA**

277 **CCCAGTTACCAATCTTGTGGACATAGATAAAGATAGTCTTGGACTTATCCATAT**

278 **GACAATAGTAAGAAAAACTTACAAGAAGACAAGAAAATTTAAAAGGATACATAT**

279 **CTCTTAAACTCTTGTCTGGT**GGCCGGCATGGTCCCAGCCTCCTCGCTGGCGCCGGC

280 TGGGCAACATTCCGAGGGGACCGTCCCCTCGGTAATGGCGAATAGCATAACCCCTT

281 GGGGCCTCTAAACGGGTCTTGAGGGGTTTTTTG.

282 The sequence of the SeV DI is highlighted in boldface.

283 Both, HCV PAMP and SeV DI RNA were purified by treatment with a 5X volume of homemade

284 solid phase reversible immobilization (SPRI) beads (comparable to Beckman-Coulter AMPure

285 beads) and elution in RNAse-free water.

286

287 Synthetic gRNAs

288 Chemically synthesized gRNAs, which were purified using high-performance liquid

289 chromatography (HPLC), were purchased from Synthego.

290

291 RNA quality control

IVT gRNAs were analyzed using a Bioanalyzer. This was performed by the UC Berkeley Functional Genomics Laboratory (FGL) core facility. gRNAs were denatured for 5 mins at 70C before analysis on bioanalyzer.

Cas9 protein preparation

The Cas9 construct (pMJ915) contained an N-terminal hexahistidine-maltose binding protein (His6-MBP) tag, followed by a peptide sequence containing a tobacco etch virus (TEV) protease cleavage site. The protein was expressed in E. coli strain BL21 Rosetta 2 (DE3) (EMD Biosciences), grown in TB medium at 16°C for 16h following induction with 0.5 mM IPTG. The Cas9 protein was purified by a combination of affinity, ion exchange and size exclusion chromatographic steps. Briefly, cells were lysed in 20 mM HEPES pH 7.5, 1M KCl, 10mM imidazole, 1 mM TCEP, 10% glycerol (supplemented with protease inhibitor cocktail (Roche)) in a homogenizer (Avestin). Clarified lysate was bound to Ni-NTA agarose (Qiagen). The resin was washed extensively with lysis buffer and the bound protein was eluted in 20 mM HEPES pH 7.5, 100mM KCl, 300mM imidazole,1 mM TCEP 10% glycerol. The His6-MBP affinity tag was removed by cleavage with TEV protease, while the protein was dialyzed overnight against 20 mM HEPES pH 7.5, 300 mM KCl, 1 mM TCEP, 10% glycerol. The cleaved Cas9 protein was separated from the fusion tag by purification on a 5 ml SP Sepharose HiTrap column (GE Life Sciences), eluting with a linear gradient of 100 mM – 1 M KCl. The protein was further purified by size exclusion chromatography on a Superdex 200 16/60 column in 20 mM HEPES pH 7.5, 150 mM KCl and 1 mM TCEP. Eluted protein was concentrated to 40uM, flash-frozen in liquid nitrogen and stored at -80°C.

315 Culture and transfection of immortalized cell lines

316 Cells were obtained from ATCC and verified mycoplasma-free (Mycoalert LT-07, Lonza).
317 HEK293, HEK293T, HCT116, HepG2 and HeLa cells were maintained in DMEM supplemented
318 with 10 % FBS and 100 µg/mL Penicillin-Streptomycin (all Gibco). K562 and Jurkat cells were
319 maintained in RPMI supplemented with 10% FBS and 100 µg/mL Penicillin-Streptomycin.
320 All transfections in cell lines were performed in 12-well cell culture dishes using $2x10^5$ cells per
321 transfection. For lipofection we used Lipofectamine™ CRISPRMAX™-Cas9, Lipofectamine®
322 RNAiMAX or Lipofectamine® 2000 Transfection Reagent (all Invitrogen) in reverse-
323 transfections according to the manufacturer's protocols. Unless stated otherwise, $2x10^5$ cells were
324 transfected with 50 pmol of RNA and harvested 24-30h post transfection for RNA extraction.
325
326 Culture and transfection of primary HSPCs
327 Human CD34+ HSPCs from mobilized peripheral blood (Allcells, Inc) were thawed and cultured
328 in StemSpan SFEM medium (StemCell Technologies) supplemented with StemSpan CC110
329 cocktail (StemCell Technologies) for 48 hours before nucleofection with dCas9 RNP (50pmol of
330 dCas9, 50 pmol of gRNA). $1.5x10^5$ HSPCs were pelleted (100 x g, 10 min) and resuspended in 20
331 µl Lonza P3 solution, mixed with 10ul dCas9 RNP, and nucleofected using ER100 protocol in
332 Lonza 4D nucleofector. Viability of the cells was measured 24 hours post nucleofection using
333 Trypan blue exclusion test. RNA was harvested 16 hours post nucleofection.
334
335 RNA extraction, cDNA synthesis and qRT-PCR
336 Cell cultures were washed with PBS prior to RNA extraction. Total RNA was extracted using
337 RNeasy Miniprep columns (Qiagen) according to the manufacturer's instructions including the

338 on-column DNAseI treatment (Qiagen). 1 µg of total RNA was used for subsequent cDNA
339 synthesis using iScript™ Reverse Transcription Supermix (Biorad). For qRT-PCR reactions, a
340 total of 20 ng of cDNA was used as a template and combined with primers (see Supplementary
341 Table 3) and SsoFast™ EvaGreen® Supermix (Biorad) and amplicons were generated using
342 standard PCR amplification protocols for 40 cycles on a StepOnePlus Real-Time PCR system
343 (Applied Biosystems). Ct values for each target gene were normalized against Ct values obtained
344 for *GAPDH* to account for differences in loading (ΔCt). To determine 'fold activation' of genes
345 ΔCt values for target genes were then normalized against ΔCt values for the same target gene for
346 mock-treated cells (ΔΔCt).
347
348 Generation of knockout cell lines
349 For CRISPR/Cas9 genome editing we used a plasmid encoding both the Cas9 protein and the
350 gRNA. pSpCas9(BB)-2A-GFP (px458) was a gift from Feng Zhang (Addgene plasmid #48138).
351 We designed gRNA sequences using the free CRISPR knockout design online tool from Synthego.
352 Two different gRNA sequences were designed for RIG-I and MDA5, respectively (see
353 Supplementary Table 3).
354 $2x10^5$ HEK293 cells were nucleofected with 2 µg of px458 plasmids containing both targeting
355 gRNAs in a 1:1 ratio using a Lonza 4D nucleofector (Lonza) with the manufacturer's
356 recommended settings. After 48h cells were harvested and subjected to fluorescence-activated cell
357 sorting (FACS). Cells expressing high levels of GFP were single-cell sorted into 96-well plates to
358 establish clonal populations.
359 For the screening process, genomic DNA from clonal populations was extracted using
360 QuickExtract solution (Lucigen). For KO of RIG-I and MDA5 we screened clones by genomic

PCR looking for a PCR product that is significantly smaller in size than that of WT HEK293 cells (see Supplementary Table 4 for primers). PCR products were then Sanger sequenced by the UC Berkeley DNA Sequencing facility using the forward primers of the PCR reaction as sequencing primers.

Western Blot

Cells were harvested and washed with PBS. Cells were lysed in 1xRIPA buffer (EMD Millipore) for 10 mins on ice. Samples were spun down at 14000xg for 15 mins and protein lysates were transferred to a new tube. 50 μg of total protein was separated for size by SDS-PAGE and transferred to a nitrocellulose membrane. Blots were blocked in 4% skim milk in 50 mm Tris-HCl (pH 7.4), 150 mm NaCl, and 0.05% Tween 20 (TBST) and then probed for RIG-I, MDA5, MAVS or GAPDH protein using antibodies against RIG-I (D14G6), MDA5 (D74E4), MAVS (D5A9E) or GAPDH (14C10), respectively (all Cell Signaling Technologies). This was followed by incubation with secondary antibody IRDye® 800CW Donkey anti-Rabbit IgG (Li-Cor). Rainbow™ protein standards (GE Healthcare) were loaded in each gel for size estimation. Blots were visualized using a Li-Cor Odyssey Clx (Li-Cor).

Acknowledgements

We would like to thank Prof. Peter Palese from the Icahn School of Medicine at Mount Sinai, New York, for the Sendai virus DI IVT template DNA. The CRISPR/Cas9 genome-editing plasmid px458 was a gift from Feng Zhang, Broad Institute, Cambridge, MA (Addgene plasmid # 48138).

References

1. Ran FA, Hsu PD, Wright J, Agarwala V, Scott DA, Zhang F. Genome engineering using the CRISPR-Cas9 system. Nat Protoc. 2013 Nov;8(11):2281–308.
2. Zhang Z, Zhang Y, Gao F, Han S, Cheah KS, Tse H-F, et al. CRISPR/Cas9 Genome-Editing System in Human Stem Cells: Current Status and Future Prospects. Mol Ther Nucleic Acids. 2017 Dec 15;9:230–41.
3. Ceasar SA, Rajan V, Prykhozhij SV, Berman JN, Ignacimuthu S. Insert, remove or replace: A highly advanced genome editing system using CRISPR/Cas9. Biochim Biophys Acta. 2016 Jun 24;1863(9):2333–44.
4. Bortesi L, Fischer R. The CRISPR/Cas9 system for plant genome editing and beyond. Biotechnol Adv. 2015 Feb;33(1):41–52.
5. Ma H, Marti-Gutierrez N, Park S-W, Wu J, Lee Y, Suzuki K, et al. Correction of a pathogenic gene mutation in human embryos. Nature. 2017 Aug 24;548(7668):413–9.
6. Gabriel R, Lombardo A, Arens A, Miller JC, Genovese P, Kaeppel C, et al. An unbiased genome-wide analysis of zinc-finger nuclease specificity. Nat Biotechnol. 2011 Aug 7;29(9):816–23.
7. Chen Y, Liu X, Zhang Y, Wang H, Ying H, Liu M, et al. A Self-restricted CRISPR System to Reduce Off-target Effects. Mol Ther. 2016;24(9):1508–10.
8. Kim S, Kim D, Cho SW, Kim J, Kim J-S. Highly efficient RNA-guided genome editing in human cells via delivery of purified Cas9 ribonucleoproteins. Genome Res. 2014 Jun;24(6):1012–9.
9. Hultquist JF, Schumann K, Woo JM, Manganaro L, McGregor MJ, Doudna J, et al. A Cas9 Ribonucleoprotein Platform for Functional Genetic Studies of HIV-Host Interactions in

406 Primary Human T Cells. Cell Rep. 2016 Oct 25;17(5):1438–52.

407 10. Schumann K, Lin S, Boyer E, Simeonov DR, Subramaniam M, Gate RE, et al. Generation
408 of knock-in primary human T cells using Cas9 ribonucleoproteins. Proc Natl Acad Sci
409 USA. 2015 Aug 18;112(33):10437–42.

410 11. DeWitt MA, Magis W, Bray NL, Wang T, Berman JR, Urbinati F, et al. Selection-free
411 genome editing of the sickle mutation in human adult hematopoietic stem/progenitor cells.
412 Sci Transl Med. 2016 Oct 12;8(360):360ra134.

413 12. Hendel A, Bak RO, Clark JT, Kennedy AB, Ryan DE, Roy S, et al. Chemically modified
414 guide RNAs enhance CRISPR-Cas genome editing in human primary cells. Nat
415 Biotechnol. 2015 Sep;33(9):985–9.

416 13. Gundry MC, Brunetti L, Lin A, Mayle AE, Kitano A, Wagner D, et al. Highly efficient
417 genome editing of murine and human hematopoietic progenitor cells by crispr/cas9. Cell
418 Rep. 2016 Oct 25;17(5):1453–61.

419 14. Dever DP, Bak RO, Reinisch A, Camarena J, Washington G, Nicolas CE, et al.
420 CRISPR/Cas9 β-globin gene targeting in human haematopoietic stem cells. Nature. 2016
421 Nov 17;539(7629):384–9.

422 15. Staahl BT, Benekareddy M, Coulon-Bainier C, Banfal AA, Floor SN, Sabo JK, et al.
423 Efficient genome editing in the mouse brain by local delivery of engineered Cas9
424 ribonucleoprotein complexes. Nat Biotechnol. 2017 May;35(5):431–4.

425 16. Charlesworth CT, Deshpande PS, Dever DP, Dejene B, Gomez-Ospina N, Mantri S, et al.
426 Identification of Pre-Existing Adaptive Immunity to Cas9 Proteins in Humans. BioRxiv.
427 2018 Jan 5;

428 17. Akira S, Uematsu S, Takeuchi O. Pathogen recognition and innate immunity. Cell. 2006

Feb 24;124(4):783–801.

18. Kell AM, Gale M. RIG-I in RNA virus recognition. Virology. 2015 May;479–480:110–21.

19. Goubau D, Schlee M, Deddouche S, Pruijssers AJ, Zillinger T, Goldeck M, et al. Antiviral immunity via RIG-I-mediated recognition of RNA bearing 5'-diphosphates. Nature. 2014 Oct 16;514(7522):372–5.

20. Saito T, Owen DM, Jiang F, Marcotrigiano J, Gale M. Innate immunity induced by composition-dependent RIG-I recognition of hepatitis C virus RNA. Nature. 2008 Jul 24;454(7203):523–7.

21. Platanias LC. Mechanisms of type-I- and type-II-interferon-mediated signalling. Nat Rev Immunol. 2005 May;5(5):375–86.

22. Milligan JF, Groebe DR, Witherell GW, Uhlenbeck OC. Oligoribonucleotide synthesis using T7 RNA polymerase and synthetic DNA templates. Nucleic Acids Res. 1987 Nov 11;15(21):8783–98.

23. Milligan JF, Uhlenbeck OC. [5] Synthesis of small RNAs using T7 RNA polymerase. RNA processing part A: general methods. Elsevier; 1989. p. 51–62.

24. Richardson CD, Ray GJ, DeWitt MA, Curie GL, Corn JE. Enhancing homology-directed genome editing by catalytically active and inactive CRISPR-Cas9 using asymmetric donor DNA. Nat Biotechnol. 2016 Mar;34(3):339–44.

25. Zuris JA, Thompson DB, Shu Y, Guilinger JP, Bessen JL, Hu JH, et al. Cationic lipid-mediated delivery of proteins enables efficient protein-based genome editing in vitro and in vivo. Nat Biotechnol. 2015 Jan;33(1):73–80.

26. Martínez-Gil L, Goff PH, Hai R, García-Sastre A, Shaw ML, Palese P. A Sendai virus-derived RNA agonist of RIG-I as a virus vaccine adjuvant. J Virol. 2013 Feb;87(3):1290–

452 300.

453 27. Horner SM, Gale M. Regulation of hepatic innate immunity by hepatitis C virus. Nat Med.
454 2013 Jul;19(7):879–88.

455 28. Diaz MO, Ziemin S, Le Beau MM, Pitha P, Smith SD, Chilcote RR, et al. Homozygous
456 deletion of the alpha- and beta 1-interferon genes in human leukemia and derived cell lines.
457 Proc Natl Acad Sci USA. 1988 Jul;85(14):5259–63.

458 29. Runge S, Sparrer KMJ, Lässig C, Hembach K, Baum A, García-Sastre A, et al. In vivo
459 ligands of MDA5 and RIG-I in measles virus-infected cells. PLoS Pathog. 2014 Apr
460 17;10(4):e1004081.

461 30. Yoneyama M, Kikuchi M, Matsumoto K, Imaizumi T, Miyagishi M, Taira K, et al. Shared
462 and unique functions of the DExD/H-box helicases RIG-I, MDA5, and LGP2 in antiviral
463 innate immunity. J Immunol. 2005 Sep 1;175(5):2851–8.

464 31. Schmidt A, Schwerd T, Hamm W, Hellmuth JC, Cui S, Wenzel M, et al. 5'-triphosphate
465 RNA requires base-paired structures to activate antiviral signaling via RIG-I. Proc Natl
466 Acad Sci USA. 2009 Jul 21;106(29):12067–72.

467 32. Hornung V, Ellegast J, Kim S, Brzózka K, Jung A, Kato H, et al. 5'-Triphosphate RNA is
468 the ligand for RIG-I. Science (80-). 2006 Nov 10;314(5801):994–7.

469 33. Chawla-Sarkar M, Lindner DJ, Liu YF, Williams BR, Sen GC, Silverman RH, et al.
470 Apoptosis and interferons: role of interferon-stimulated genes as mediators of apoptosis.
471 Apoptosis. 2003 Jun;8(3):237–49.

472 34. Onomoto K, Yoneyama M, Fung G, Kato H, Fujita T. Antiviral innate immunity and stress
473 granule responses. Trends Immunol. 2014 Sep;35(9):420–8.

474 35. Yu Q, Katlinskaya YV, Carbone CJ, Zhao B, Katlinski KV, Zheng H, et al. DNA-damage-

induced type I interferon promotes senescence and inhibits stem cell function. Cell Rep. 2015 May 5;11(5):785–97.

36. Pietras EM, Lakshminarasimhan R, Techner J-M, Fong S, Flach J, Binnewies M, et al. Re-entry into quiescence protects hematopoietic stem cells from the killing effect of chronic exposure to type I interferons. J Exp Med. 2014 Feb 10;211(2):245–62.

37. de Weerd NA, Samarajiwa SA, Hertzog PJ. Type I interferon receptors: biochemistry and biological functions. J Biol Chem. 2007 Jul 13;282(28):20053–7.

38. Kim S, Koo T, Jee H-G, Cho H-Y, Lee G, Lim D-G, et al. CRISPR RNAs trigger innate immune responses in human cells. Genome Res. 2018 Feb 22;

39. Lorenz R, Bernhart SH, Höner Zu Siederdissen C, Tafer H, Flamm C, Stadler PF, et al. ViennaRNA Package 2.0. Algorithms Mol Biol. 2011 Nov 24;6:26.

488

Figure 1

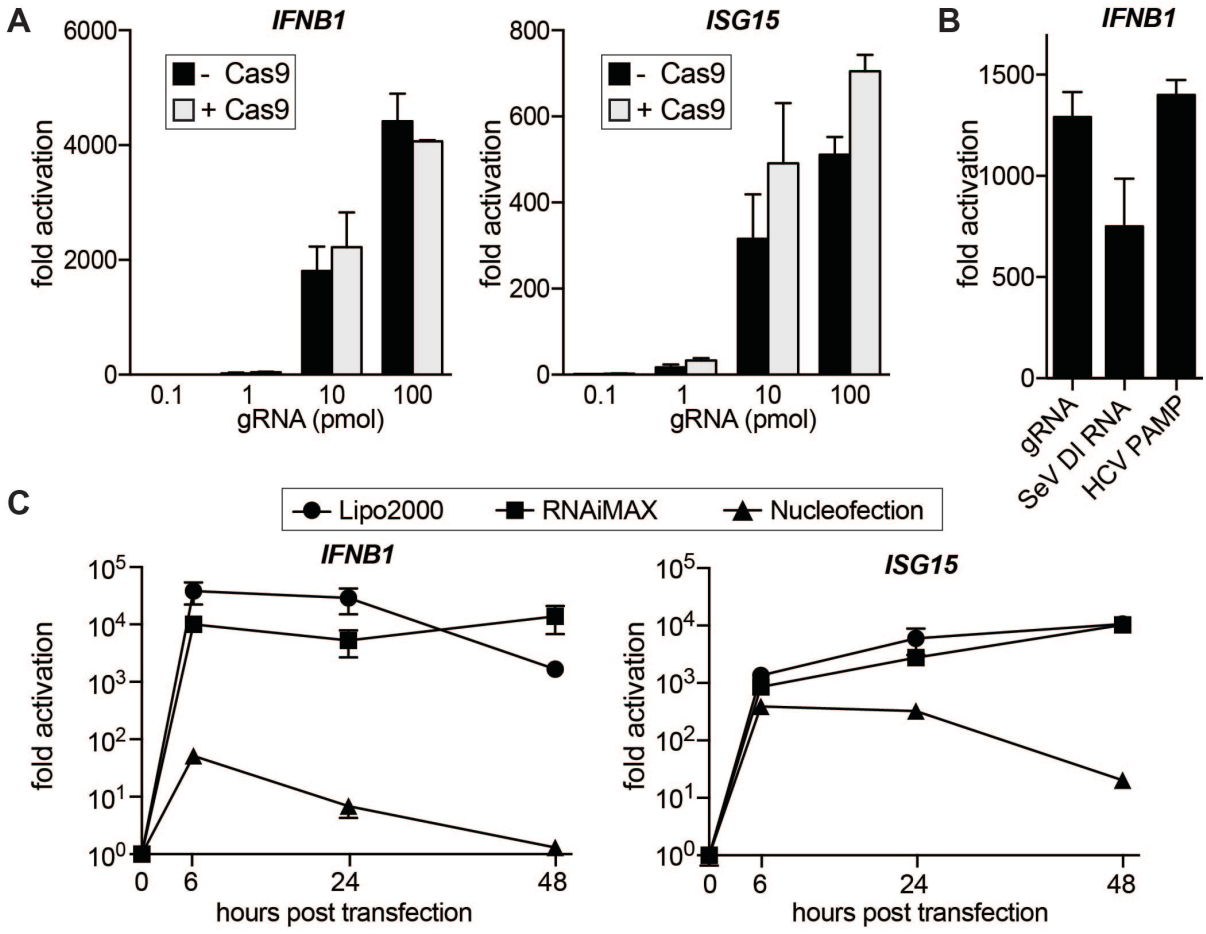

489

490 **Figure 1: Transfection of IVT gRNAs into HEK293 cells triggers a type I interferon response.**

491 (**A**) qRT-PCR analysis of *IFNB1* and *ISG15* transcript levels in HEK293 cells transfected with

492 increasing amounts of gRNA with and without Cas9 protein. In the samples with Cas9, gRNAs

493 were complexed with constant amounts (100 pmol) of Cas9 protein. Cells were harvested for RNA

494 extraction 30h after transfection using CRISPRMAX transfection reagent. Ct values were

495 normalized to Ct values of mock transfected HEK293 cells to determine fold activation. (**B**) qRT-

496 PCR analysis of *IFNB1* transcript levels in HEK293 cells transfected with equimolar amounts (50

497 pmol) of IVT gRNA, Sendai Virus defective interfering (SeV DI) RNA or HCV PAMP,

498 respectively. (**C**) qRT-PCR analysis of *IFNB1* and *ISG15* transcript levels in HEK293 cells over a
499 48h time course after transfection with 50 pmol via lipofection (Lipofectamine2000 or
500 RNAiMAX) or nucleofection, respectively. For all panels average values of three biological
501 replicates +/-SD are shown.
502

Figure 2

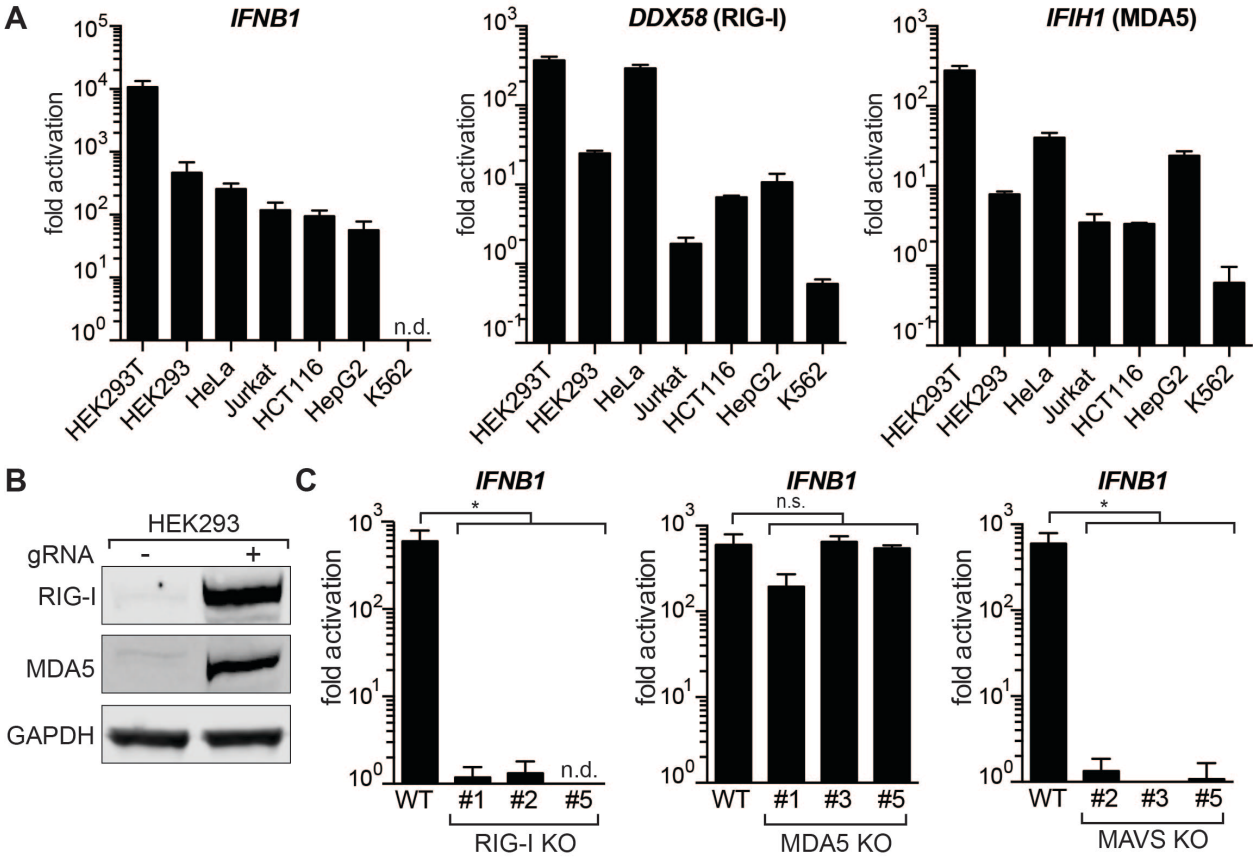

503

504 **Figure 2: IVT gRNAs are recognized via the RIG-I pathway.** (**A**) qRT-PCR analysis of increase
505 in *IFNB1* transcript levels (left) and transcript levels of the two main cytosolic RIG-I-like receptors
506 (*DDX58* and *IFIH1*) after introduction of IVT gRNA. Cell lines were ordered by responsiveness
507 to gRNA-mediated induction of *IFNB1* transcript levels. Cells were harvested for RNA extraction
508 30h after transfection. Ct values were normalized to Ct values of mock transfected cells for each

509 cell line to determine fold activation. *IFNB1* levels for K562 cells were too low to be determined
510 (n.d.). (**B**) Western Blot analysis for RIG-I and MDA5 expression of mock transfected and gRNA
511 transfected HEK293 cells after 48h. (**C**) qRT-PCR analysis of *IFNB1* transcript levels in HEK293
512 RIG-I (left), MDA5 (middle) and MAVS (right) knockout cells. Shown are three biological
513 replicates of three clonal populations of RIG-I, MDA5 or MAVS KO cells, respectively. *IFNB1*
514 levels for RIG-I KO clone #5 were too low to be determined (n.d.). For panels A and C, cells were
515 harvested for RNA extraction 30h after transfection using RNAiMAX transfection reagent.
516 Average values of three biological replicates +/-SD are shown. Statistical significances were
517 calculated by unpaired t-test (*p<0.0001, n.s.: not significant).
518

Figure 3

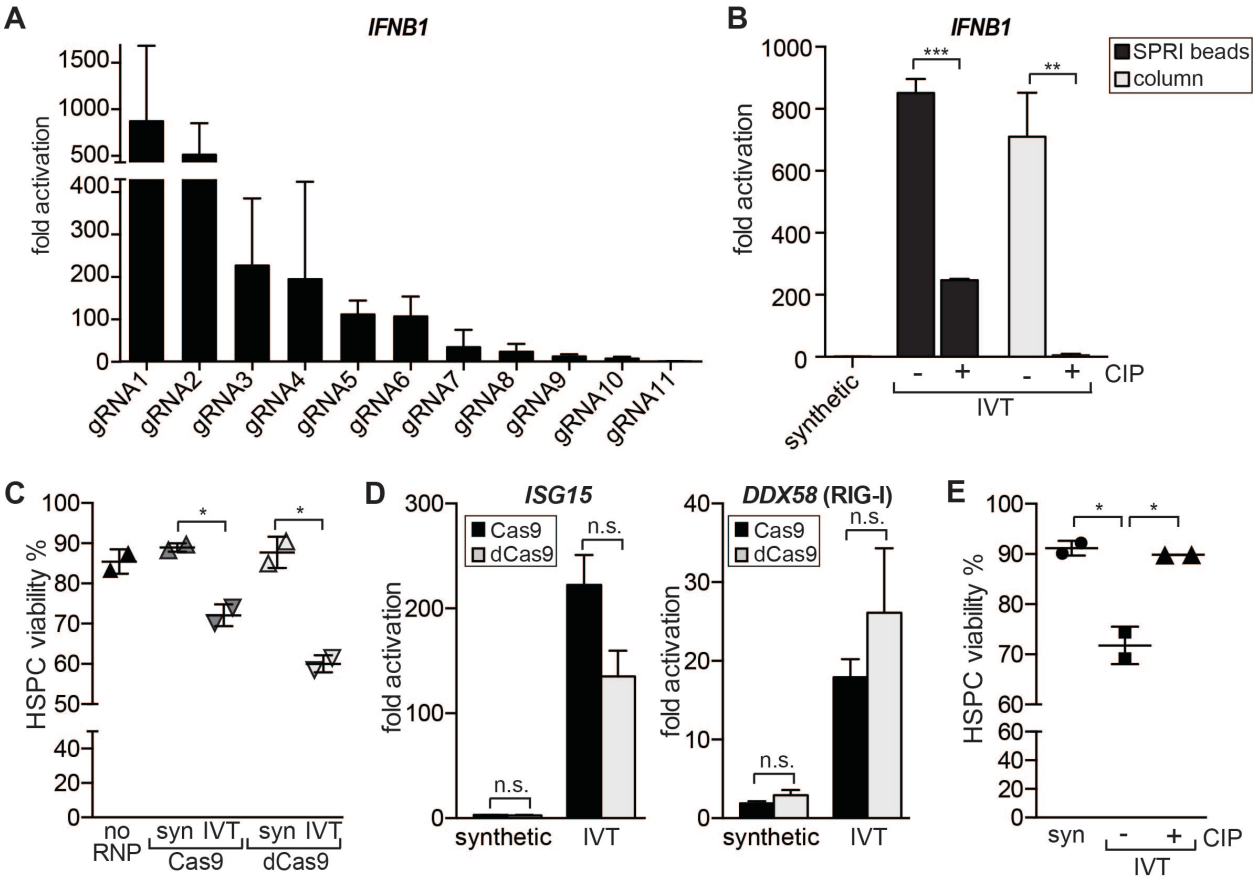

519

520 **Figure 3. Protospacer and 5'-triphosphate determine the intensity of the gRNA-mediated**

IFNβ response. (**A**) qRT-PCR analysis of *IFNB1* transcript levels in HEK293 cells transfected with equal amounts of gRNAs containing different 20 nucleotide protospacers. gRNAs were ordered by decreasing levels of *IFNB1* activation. gRNA1 refers to the gRNA that has been used in all previous experiments. (**B**) qRT-PCR analysis of *IFNB1* transcript levels in HEK293 cells transfected with synthetic, IVT and Calf intestine phosphatase treated (CIP) IVT gRNAs (gRNA1). After IVT and CIP treatment gRNAs were purified with SPRI beads or spin columns, respectively. Cells were harvested for RNA extraction 30h after transfection with RNAiMAX transfection reagent. Average values of three biological replicates +/-SD are shown. (**C**) Viability of human primary HSPCs 24h post nucleofection with no RNP and Cas9 or dCas9 RNPs. dCas9 or Cas9 were complexed with synthetic (syn) or IVT gRNA targeting the *HBB* gene. Viability was determined by Trypan blue exclusion test. (**D**) qRT-PCR analysis of *ISG15* and *DDX58* (RIG-I) transcript levels in human primary HSPCs 16h post nucleofection. dCas9 or Cas9 were complexed with synthetic or IVT gRNA targeting the *HBB* gene, respectively. Ct values were normalized against Ct of mock-nucleofected cells. Average values of two biological replicates +/-SD are shown. (**E**) Viability of human primary HSPCs 16h post transfection with RNPs. RNPs consisted of dCas9 complexed with synthetic, IVT or CIP-treated IVT gRNAs targeting a non-coding intron of *JAK2*. Viability was determined by Trypan blue exclusion test. Statistical significances were calculated by unpaired t-test (*$p<0.05$, **$p<0.01$, ***$p<0.0001$, n.s.: not significant).

540

Figure 4

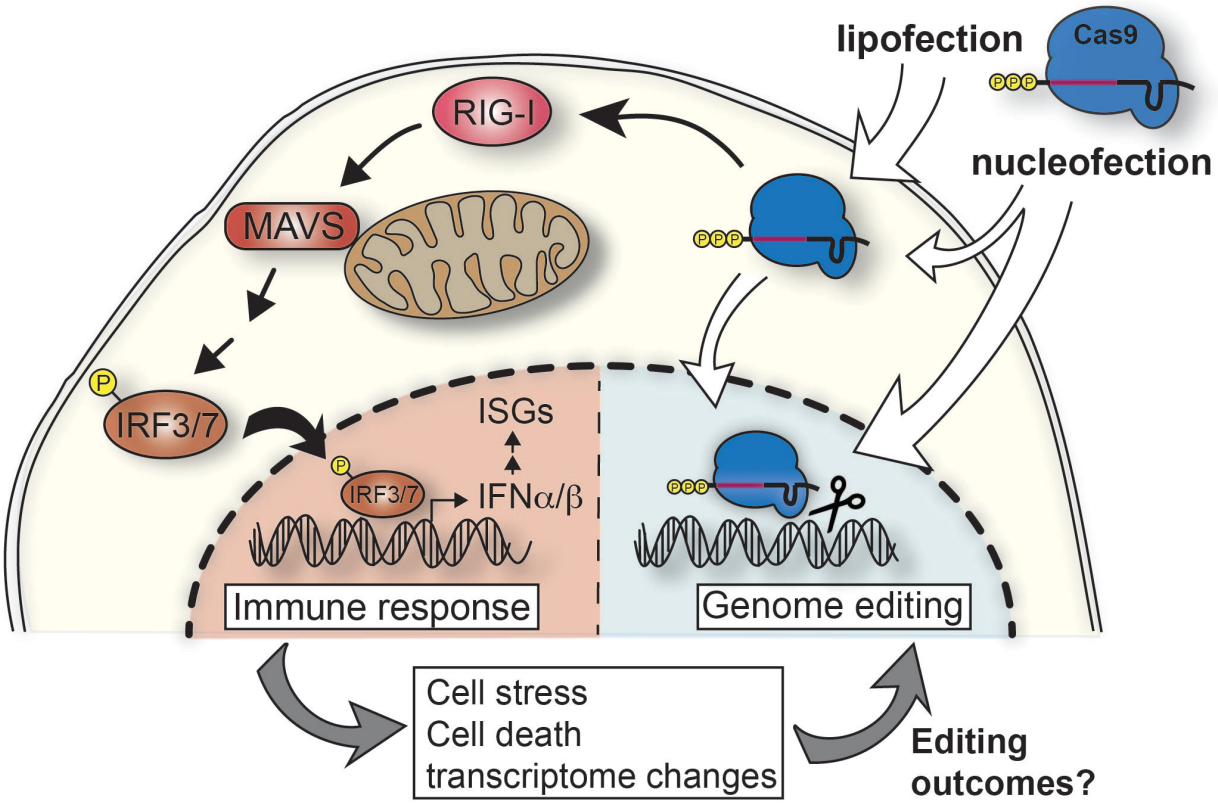

541

542 **Figure 4. Transfection of *in vitro* transcribed gRNAs induces a cytosolic immune response.**

543 Proposed model of IVT gRNA recognition pathways in mammalian cells. IVT gRNAs carry a 5'-

544 triphosphate and when complexed with Cas9 protein and transfected into cells, cytosolic RNPs are

545 recognized by RIG-I triggering a cascade of activation events through the mitochondrial antiviral

546 signaling protein (MAVS). This results in phosphorylation of IRF3/7 and their shuttling into the

547 nucleus to activate expression of type I interferons (IFNα/β). This triggers the expression of

548 interferon-stimulated genes (ISGs). This innate immune response changes the transcriptome of the

549 cell and can cause cell stress and/or death which in turn might affect the editing outcomes.

550